PROCEEDINGS
OF SCIENCE

Recent QCD results from the xFITTER project:

Probing the strange content of the proton with charm production in charged current at LHeC

The xFITTER Developers' Team:[∗] **Hamed Abdolmaleki,**[a] **Valerio Bertone,**[b]
Daniel Britzger,[c] **Stefano Camarda,**[d] **Amanda Cooper-Sarkar,**[e] **Achim Geiser,**[f]
Francesco Giuli,[g] **Alexander Glazov,**[f] **Agnieszka Luszczak,**[h] **Ivan Novikov,**[i]
Fred Olness,[j][†] **Andrey Sapronov,**[i] **Oleksandr Zenaiev,**[k]

[a] *Faculty of Physics, Semnan University, 35131-19111 Semnan, Iran*

[b] *Dipartimento di Fisica, Università di Pavia and INFN, Sezione di Pavia Via Bassi 6, I-27100 Pavia, Italy*

[c] *Max-Planck-Institut für Physik, Föhringer Ring 6, D-80805 München, Germany*

[d] *CERN, CH-1211 Geneva 23, Switzerland*

[e] *Particle Physics, Denys Wilkinson Bdg, Keble Road, University of Oxford, OX1 3RH Oxford, UK*

[f] *Deutsches Elektronen-Synchrotron (DESY), Notkestrasse 85, D-22607 Hamburg, Germany*

[g] *University of Rome Tor Vergata and INFN, Sezione di Roma 2, Via della Ricerca Scientifica 1, 00133 Rome, Italy*

[h] *T. Kosciuszko Cracow University of Technology, PL-30-084, Cracow, Poland*

[i] *Joint Institute for Nuclear Research, Joliot-Curie 6, Dubna, Moscow region, Russia, 141980*

[j] *SMU Physics, Box 0175 Dallas, TX 75275-0175, USA*

[k] *Hamburg University, II. Institute for Theoretical Physics, Luruper Chaussee 149, D-22761 Hamburg, Germany*

We investigate charm production in charged-current deep-inelastic scattering (DIS) using the xFITTER program. xFITTER is an open-source software framework for the determination of PDFs and the analysis of QCD physics, and has been used for a variety of LHC studies. The study of charged current DIS charm production provides an important perspective on the strange quark PDF, $s(x)$. We make use of the xFITTER tools to study the present $s(x)$ constraints, and then use LHeC pseudodata to infer how these might improve. Furthermore, as xFITTER implements both Fixed Flavor and Variable Flavor number schemes, we can examine the impact of these different theoretical choices; this highlights some interesting aspects of multi-scale calculations. This study provides a practical illustration of the many features of xFitter.

XXVII International Workshop on Deep-Inelastic Scattering and Related Subjects - DIS2019
8-12 April, 2019
Torino, Italy

1. xFITTER Overview

The Parton Distribution Functions (PDFs) are the essential components that allow us to make theoretical predictions for experimental measurements of hadrons. The precision of the PDF analysis has advanced tremendously in recent years, and these studies are now performed with very high precision at NLO and NNLO in perturbation theory. The xFITTER project[1] is an open source QCD fit framework that can perform PDF fits, assess the impact of new data, compare existing PDF sets, and perform a variety of other tasks [1]. The modular structure of xFITTER allows for interfaces to a variety of external programs including: QCDNUM [4], APFEL [5], LHAPDF [6], APPLGRID [7], APFELGRID [8], FastNLO [9] and HATHOR [10].

An overview of the recent xFITTER updates and available tutorials is available in Ref. [11]. In this short report we will focus on the charged current (CC) production of charm and the impact on the underlying strange quark PDF [2].

2. Charged Current (CC) Charm Production and the LHeC

In this study, we will examine the charged current (CC) production of charm to provide insight on the underlying strange quark PDF. The strange quark PDF has been extensively investigated in a number of experiments including fixed-target neutrino/antineutrino-nucleon DIS experiments, and the associated production of a W boson with a charm-jet final state at the LHC. Despite these measurements, $s(x)$ still has a sizable uncertainty; in the future it is essential to reduce this uncertainty as we strive to make increasingly precise tests of the SM and search for what might lie beyond.

The proposed Large Hadron Electron Collider (LHeC) facility can provide high statistics measurements of electrons on both protons and nuclei across a broad kinematic range to address many of these outstanding questions [12]. For example, a 7 TeV proton beam on a 60 GeV electron beam could provide $\sqrt{s} \sim 1.3$ TeV. Compared to HERA, the LHeC extends the covered kinematic range by an order of magnitude in both x_{Bj} and Q^2 with a nominal design luminosity of $10^{33}cm^{-2}s^{-1}$.

Specifically, the process we'll consider is $Ws \rightarrow c$ at leading-order (LO); higher-order corrections include $Wg \rightarrow c\bar{c}$ and $Wc \rightarrow c\bar{s}$. This process touches on a number of interesting QCD aspects. It is a multi scale problem as it involves the boson mass M_W and Q^2 scale in addition to the quark masses $\{m_s, m_c\}$. Additionally, because we have possible contributions from a charm PDF at NLO, we can choose to compute this in either the Variable Flavor Number Scheme (VFNS) or a Fixed Flavor Number Scheme (FFNS) As xFITTER has both VFNS and FFNS implemented, we find it useful to compare these two perspectives.

3. The VFNS and FFNS

In Fig. 1 we display the ratio for NLO CC charm production computed in the VFNS (using the FONLL-B calculation with the NPDF3.1 NLO PDF set), and in the FFNS (using the FFNS A calculation with the ABMP16 NLO PDF set). Examining Fig. 1-a) we observe that the VFNS and

---

[1]xFitter can be downloaded from `www.xFitter.org`. An overview of the program can be found in Ref. [1]. A more extensive report of these features can be found in Ref. [2]. Also see the recent study of Ref. [3].
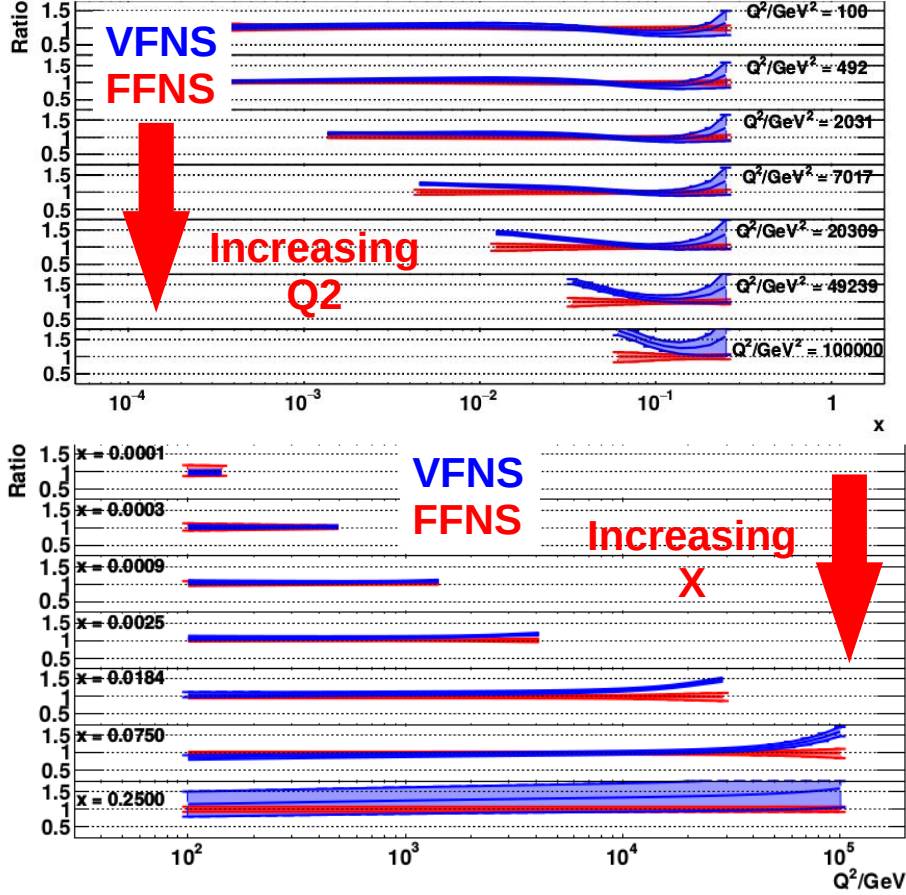
Figure 1: Comparison of the theoretical predictions (ratio) with uncertainties for CC charm production at the LHeC vs. x_{bj} (top) and Q^2 (bottom) as calculated in the FFNS (FFNS A) and VFNS (FONLL-B) context. We observe increasing differences at large Q^2 and large x_{bj} values.[2]

FFNS yield comparable results throughout the x range for lower Q^2 values, but differ for increasing Q^2. Correspondingly, in Fig. 1-b) the differences increase for the larger x values [2].

Q^2 **Dependence:** To better understand the relative behavior of the FFNS and VFNS calculations, we recall that when the scale $Q \sim \mu$ is below the charm PDF matching scale μ_c (typically taken to be equal to m_c [13]) the charm PDFs vanish and the FFNS and VFNS reduce to the same result.[2] For increasing Q scales, the VFNS resums the $\alpha_S \ln(Q^2/m_c^2)$ contributions via the DGLAP evolution equations and the FFNS and VFNS will slowly diverge logarithmically. This behavior is observed in Fig. 1 and is consistent with the characteristics demonstrated in Ref. [14]. Thus, we have identified the source of the scheme differences at large Q^2.

x **Dependence:** The source of the scheme differences at large x is a bit more intricate. The VFNS uses the DGLAP equations to resum higher-order logarithms of the form $\alpha_S \ln(Q^2/m_c^2)$, and these are balanced with the counter-terms of the NLO contributions. Thus, the net contribution of the VFNS over the FFNS depends on the particular value of x, and we find (c.f., Fig. 11 of Ref. [14].) that these terms increase for larger x values. Thus, we have identified the source of the scheme differences at large x.

---

[2]Note,we note the PDF uncertainties are taken from the separate underlying PDF sets with their distinctive methodologies and cannot be directly compared.
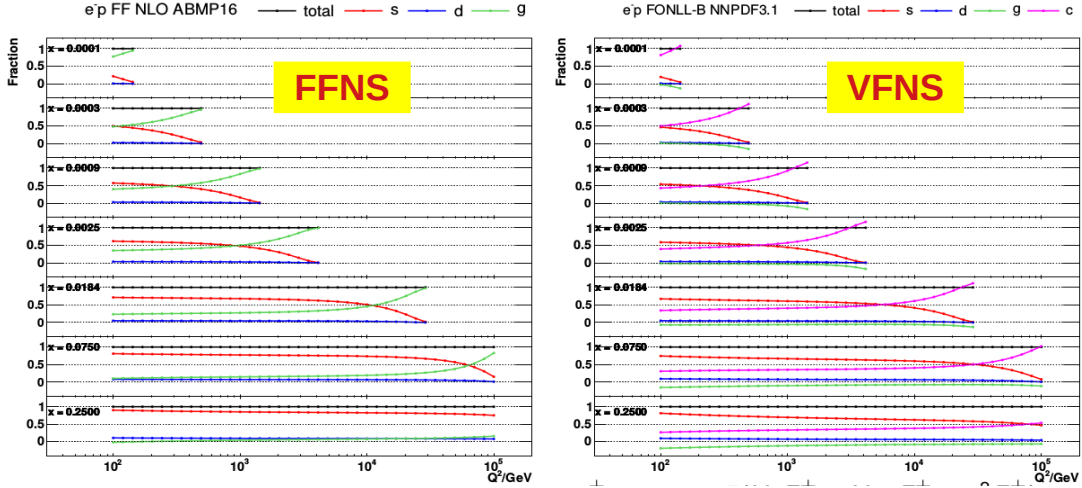
Figure 2: The partonic subprocesses for charm CC production cross sections for FFNS (FFNS A) and VFNS (FONLL-B) as a function of Q^2 for different values of x_{bj}, Ref. [2].

4. Flavor Decomposition

In Fig. 2 we display the separate partonic contributions to the total cross section as a function of $\{x, Q^2\}$ in both the FFNS and VFNS. We find it very interesting that the charm contribution in the VFNS (magenta line) is remarkably similar to the gluon contribution in the FFNS (green line). In the FFNS decomposition, we note that the charm component is not present by definition as the charm PDF is not included in this framework; charm can only enter here via an external gluon splitting process $g \to c\bar{c}$.

In contrast, in the VFNS the charm component is present, and mainly produced by $g \to c\bar{c}$ collinear splitting through DGLAP evolution. The fundamental underlying process is (and has to be) the same in both the FFNS and VFNS, but the factorization boundary between PDFs and hard scattering cross section (determined by the scale μ and the scheme choice) is different. This behavior underscores the fact that the renormalization scale μ is simply "shuffling" contributions among the separate sub-pieces, but the total physical cross section remains positive and stable, *cf*. Refs. [2, 14]. This is a triumph of the QCD theory.

Next, turning our attention to the strange PDF contribution, we observe that the FFNS and VFNS predictions behave qualitatively very similar as functions of the kinematic variables. Specifically, the strange fraction increases for x_{Bj} and decreases for Q^2 and y. In particular, at high y the strange PDF contribution drops to zero in favor of the gluon or charm quark PDFs. In these phase-space regions, the dominant contributions to the cross section are proportional to the gluon PDF in the FFNS or to the charm-quark PDFs in the VFNS.

Finally, we add that the XFITTER 2.0.0 program links to the APFEL code [5] which has implemented generalized matching conditions that enable the switch from NF to NF +1 active flavors at an arbitrary matching scale μ_m. This enables us to generalize the transition between a FFNS and a VFNS and essentially vary continuously between the two schemes; in this sense the matching scale μ_m allows us to unify the FFNS and VFNS in a common framework [13].

3
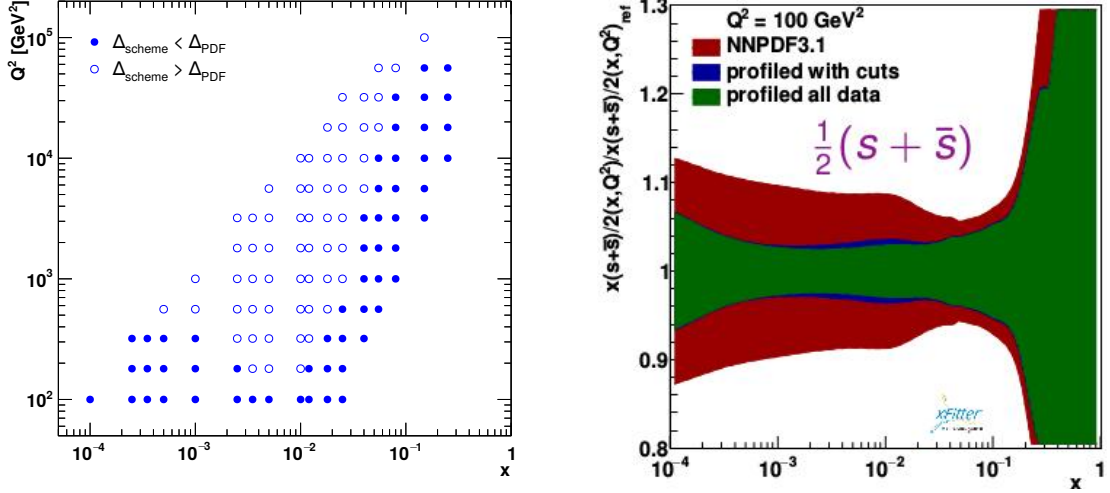
(a) The full ($\Delta_{\text{scheme}} < \Delta_{\text{PDF}}$, $\Delta_{\text{scheme}} > \Delta_{\text{PDF}}$) and restricted ($\Delta_{\text{scheme}} < \Delta_{\text{PDF}}$) sets of data points which are used for PDF profiling.

(b) The relative strange quark PDF uncertainties at Q^2=100 GeV^2 of the original and profiled NNPDF3.1 PDF set.

Figure 3: LHeC Constraints on the Strange PDF, *c.f.*, Ref. [2].

5. LHeC Constraints on the Strange PDF

Having outlined the theoretical ingredients we now assess the ability of the LHeC to constrain the PDFs. We use pseudodata for differential CC charm production cross sections in Q^2 and x_{Bj} corresponding to an integrated luminosity of 100 fb^{-1} and polarization $P = -0.8$. The charm-mass reference value in the $\overline{\text{MS}}$ scheme is set to $m_c(m_c) = 1.27$ GeV and α_s is set to the value used for the corresponding PDF extraction. The renormalization and factorization scales are chosen to be $\mu_{\text{r}}^2 = \mu_{\text{f}}^2 = Q^2$. Details are provided in Ref. [2].

We have observed in the previous discussion that the VFNS and FFNS can differ across the $\{x, Q^2\}$ kinematic plane. This is illustrated in Fig. 3a where the open data points indicate where the difference between the VFNS and FFNS is larger than the PDF uncertainty, $\Delta_{\text{scheme}} > \Delta_{\text{PDF}}$. To gauge the impact of this heavy flavor scheme choice, we will therefore perform the profiling study of the PDFs with i) the full set of LHeC pseudodata, and ii) the restricted set (with cuts) where the difference between the VFNS and FFNS is smaller than the PDF uncertainty, $\Delta_{\text{scheme}} < \Delta_{\text{PDF}}$ (solid data points.). This latter profiled PDF will provide a conservative estimate that is independent of the particular VFNS or FFNS,

In Fig. 3b we display the strange PDF uncertainty for the the original PDF set, the profiled PDF set with the all data, and with the PDF with the restricted data set with cuts. For both LHeC data sets, the reduction in $s(x)$ is dramatic in the intermediate to low x region; this is encouraging as it demonstrates the LHeC will have significant impact on the strange PDF across a broad kinematic region. Additionally, we note that the difference between the full data and the restricted data is minimal; hence, any uncertainty arising from the VFNS/FFNS choice has a negligible impact on the final PDF.

6. Conclusion

The XFITTER 2.0.0 program is a versatile, flexible, modular, and comprehensive tool that can facilitate analyses of the experimental data and theoretical calculations. In this study we have examined the ability of CC charm production data at the LHeC to constraint the PDF uncertainty. This project demonstrates a number of the XFITTER features including the ability to compute in both the VFNS and the FFNS. This feature, in addition to the variable heavy flavor matching scale μ_m, allow us to generalize the transition between a VFNS and a FFNS, and provides a theoretical "laboratory" which can quantitatively explore aspects of the QCD theory. We have decomposed the separate flavor components contributing to the process, and studied the effects of the VFNS and FFNS across the $\{x, Q^2\}$ kinematic plane.

Finally, we use the profiling ability of XFITTER to investigate the impact of the LHeC pseudodata and find this can dramatically improve the PDF uncertainty *independent* of the underlying heavy flavor scheme used in the calculation. This study not only provides new insights into the intricacies of QCD, but also has practical advantages for PDF fits and future facilities.

References

[1] S. Alekhin et al. "HERAFitter". In: *Eur. Phys. J.* C75.7 (2015), p. 304. arXiv: `1410.4412 [hep-ph]`.

[2] Hamed Abdolmaleki et al. "Probing the strange content of the proton with charm production in charged current at LHeC". In: (2019). arXiv: `1907.01014 [hep-ph]`.

[3] Rabah Abdul Khalek et al. "Probing Proton Structure at the Large Hadron electron Collider". In: (2019). arXiv: `1906.10127 [hep-ph]`.

[4] M. Botje. "QCDNUM: Fast QCD Evolution and Convolution". In: *Comput. Phys. Commun.* 182 (2011), pp. 490–532. arXiv: `1005.1481 [hep-ph]`.

[5] Valerio Bertone, Stefano Carrazza, and Juan Rojo. "APFEL: A PDF Evolution Library with QED corrections". In: *Comput. Phys. Commun.* 185 (2014), pp. 1647–1668. arXiv: `1310.1394 [hep-ph]`.

[6] Andy Buckley et al. "LHAPDF6: parton density access in the LHC precision era". In: *Eur. Phys. J.* C75 (2015), p. 132. arXiv: `1412.7420 [hep-ph]`.

[7] Tancredi Carli et al. "A posteriori inclusion of parton density functions in NLO QCD final-state calculations at hadron colliders: The APPLGRID Project". In: *Eur. Phys. J.* C66 (2010), pp. 503–524. arXiv: `0911.2985 [hep-ph]`.

[8] Valerio Bertone, Stefano Carrazza, and Nathan P. Hartland. "APFELgrid: a high performance tool for parton density determinations". In: *Comput. Phys. Commun.* 212 (2017), pp. 205–209. arXiv: `1605.02070 [hep-ph]`.

[9] Daniel Britzger et al. "New features in version 2 of the fastNLO project". In: *Proceedings, 20th International Workshop on Deep-Inelastic Scattering and Related Subjects (DIS 2012): Bonn, Germany, March 26-30, 2012*. 2012, pp. 217–221. arXiv: `1208.3641 [hep-ph]`.

[10] M. Aliev et al. "HATHOR: HAdronic Top and Heavy quarks crOss section calculatoR". In: *Comput. Phys. Commun.* 182 (2011), pp. 1034–1046. arXiv: `1007.1327 [hep-ph]`.

[11] V. Bertone et al. "xFitter 2.0.0: An Open Source QCD Fit Framework". In: *PoS* DIS2017 (2018), p. 203. arXiv: `1709.01151 [hep-ph]`.

[12] J. L. Abelleira Fernandez et al. "A Large Hadron Electron Collider at CERN: Report on the Physics and Design Concepts for Machine and Detector". In: *J. Phys.* G39 (2012), p. 075001. arXiv: `1206.2913 [physics.acc-ph]`.

[13] V. Bertone et al. "Impact of the heavy quark matching scales in PDF fits". In: *Eur. Phys. J.* C77.12 (2017), p. 837. arXiv: `1707.05343 [hep-ph]`.

[14] A. Kusina et al. "Hybrid scheme for heavy flavors: Merging the fixed flavor number scheme and variable flavor number scheme". In: *Phys. Rev.* D88.7 (2013), p. 074032. arXiv: `1306.6553 [hep-ph]`.